Journal of Energy Storage 22 (2019) 144–152

Contents lists available at ScienceDirect

Journal of Energy Storage

journal homepage: www.elsevier.com/locate/est

Optimal management of electric vehicles in an intelligent parking lot in the presence of hydrogen storage system

Reza Razipour[a], Seyed-Masoud Moghaddas-Tafreshi[a,*], Payam Farhadi[b]

[a] Department of Electrical Engineering, Faculty of Engineering, University of Guilan, Rasht, Iran
[b] Young Researchers and Elite Club, Parsabad Moghan Branch, Islamic Azad University, Parsabad Moghan, Iran

ARTICLE INFO

Keywords:
Optimal operation
Plug-in hybrid electrical vehicle
Intelligent parking lot
Smart grid
Hydrogen storage system

ABSTRACT

Charging/discharging management of electric vehicles (EVs) and dispatch of intermittent renewable energies will be probably two significant issues in future distribution system operation and planning. In addition, intelligent parking lots (IPLs) are widely employed due to ever-increasing number of EVs. In this paper, a novel stochastic approach is proposed for charging/discharging management of EVs parked in IPLs where the electric vehicles are interacting with each other and the upstream grid operator. A newly developed model is presented for the intelligent parking lot with hydrogen storage system (HSS) consisting of fuel cell, electrolyzer, and hydrogen storage tank as well as load demand in which practical constraints are satisfied. The costs of operation related to distribution system, including the purchasing cost of energy from upstream grid and the cost of EVs charging in IPLs, are formulated as the most important objectives of the proposed optimization problem. Particle swarm optimization (PSO) algorithm as a fast and population-based technique was carried out in simulations. And, based on the obtained simulation results, all technical and financial objectives are achieved.

1. Introduction

The ever-increasing fossil-fuel depletion and environmental issues have long been strong motivations behind interests in application of electric vehicles (EVs) throughout the world because EVs are a good solution toward CO_2 emission reduction if they are utilized optimally in exchangeable modes of energy storage and/or electric load. However, application of large number of EVs as the mass electric loads to power systems may lead to significant challenges. Furthermore, the use of hydrogen as a clean and abundant alternative for fueling the transportation sector is considered. When hydrogen is consumed, the bi-product will be almost only water vapor that is why it is one of the environmentally-friendly promises considered for near future mass-consumptions. Hydrogen can be used as a very useful fuel for electric and nonelectric vehicles, fixed and mobile power stations and transportation [1]. Local generation units based on renewable and/or non-renewable energy resources and energy storage systems with the ability of producing local power may be employed in microgrids (MGs) based on smart technology to meet growing energy demand. The widely utilized generation units can be photovoltaics (PVs), wind turbines (WTs), microturbines (MTs), and fuel cells (FCs) [2–7].

Generally, energy storage systems may be classified with regard to the type of energy conversion into four groups: mechanical systems, electrical systems, electrochemical systems (batteries), and hydrogen storage. The hydrogen storage system principle is based on the conversion of electricity to hydrogen in charging mode and the conversion of hydrogen to electricity in the discharge stage.

In order to make hydrogen gas accessible, separate water molecules are needed. Every water molecule includes two atoms of hydrogen and one atom of oxygen. Thus, a unique process called electrolysis is applied to break down water molecule into its building blocks (i.e., hydrogen and oxygen). In the first step, hydrogen is obtained through water electrolysis where water is further decomposed into oxygen and hydrogen. And then, the process is followed by electrical energy conversion using an internal combustion engine or a fuel cell [8]. One of the remarkable advantages of the hydrogen storage system (from economical view points) is to store energy (H_2) during off-peak period when electricity tariff is low and supply outweigh the demand and, then, convert H_2 to electrical energy by fuel cells in peak period when electricity tariff is high [9]. Hydrogen storage technology is a fundamental requirement for the implementation of energy systems based on the hydrogen technology that is essential for the development of the hydrogen energy economy [8,10]. The traditional storage of hydrogen in the form of a gas requires a lot of pressure to compress hydrogen. So, the nanosystems with high electrochemical discharge capacity are used to store hydrogen. Hydrogen can be stored either at the surface of the

* Corresponding author.
E-mail address: tafreshi@guilan.ac.ir (S.-M. Moghaddas-Tafreshi).

https://doi.org/10.1016/j.est.2019.02.001
Received 18 November 2018; Received in revised form 26 January 2019; Accepted 1 February 2019

Nomenclature

A	Initial investment cost
CF	Capacity factor
EV	Electric vehicles
FC	Fuel cell
GA	Genetic algorithm
G2V	Grid-to-vehicle
HSS	Hydrogen storage system
IPL	Intelligent parking lots
MT	Microturbine
MCS	Monte Carlo simulation
n	Lifetime
PHEV	Plug-in hybrid electrical vehicles
PSO	Particle swarm optimization
PV	Photovoltaics
RES	Renewable energy resources
SOC	State of charge
V2G	Vehicle-to-grid
WT	Wind turbines
C^v	Capacity of the battery
C_{EL}	Operation cost of the electrolyzer
C_{FC}	Operation cost of the fuel cell
P^t_{FC-IPL}	Power transferred from the fuel cell to the IPL
P^t_{IPL-EL}	Electrical power delivered to the electrolyzer from the IPL
P^t_{grid}	Power exchanged with the upstream grid
P_{grid_max}	Maximum capacity of the transmission line connected to the upstream grid
P^{max}_{EL}	Maximum power of the electrolyzer
P^{max}_{FC}	Maximum power of the fuel cell
P_{rated}	Rated power of each component
P^t	Actual power of each component
$P^{max}_{v.c}$	Maximum charging power of the charger
$P^{max}_{v.d}$	Maximum discharging power of the charger
P^t_H	Power exchanged with the hydrogen unit
$P^t_{sell-grid}$	Power sold to the upstream grid
$P^t_{v.c}$	Charging power of the battery
$P^t_{v.d}$	Discharging power of the battery
$SOC_{t^d_v}$	Final SOC of the vehicle
$SOC_{t^a_v}$	Initial SOC of the vehicle
C_M	Maintenance cost
C_{Tank}	Operation cost hydrogen tank
E_{H_2}	Hydrogen energy
M_{max}	Maximum capacity of the hydrogen tank
M^t_{Tank}	Hydrogen mass stored in the tank in period t
$M^{t-\Delta t}_{Tank}$	Hydrogen mass stored in the tank in period t-Δt
m_{V2G}	Set of V2G vehicles
$P^t_{buy-grid}$	Power purchased from the upstream grid
P^t_L	Electrical load in period t
P^t_c	Sum of the charging power of all the PHEVs in period t
P^t_d	Sum of the discharging power of all the PHEVs in period t
$P^t_{EL-Tank}$	Output power of the electrolyzer in every period t
$SOC^{desired}_v$	Desired final SOC of the vehicle
t^a_v	Arrival time
t^d_v	Departure time
Λ^t_v	A binary variable indicating connection state of the vehicle in every period
τ^d_v	A flag indicating the departure time of the vehicle
η_{EL}	Electrolyzer efficiency
η_{FC}	Fuel cell efficiency
η^v_c	Charging efficiency of the battery
η^v_d	Discharging efficiency of the battery
η_{Tank}	Efficiency of the tank
γ	Interest rate
ρ^t_c	Charging price of the vehicle in period t
$\rho^t_{c.V2G}$	Charging price of the V2G vehicle in period t
$\rho^t_{d.V2G}$	Discharging price of the V2G vehicle in period t
$\rho^t_{sell-load}$	Price at which the IPL sells energy to its loads.
Δt	Length of each period

solids (physisorption) or inside them (chemisorption). There are various materials that can absorbed hydrogen, including: alloys and alloy hydrides, (mixed) metal oxides, metal-organic frameworks, carbon and graphemes [1]. In Rf. [10], the design of new nanocomposites for electrochemical hydrogen storage, with emphasis on optimization, have been proposed to achieve higher performance superior to other nanocomposites.

EVs are designed for different type of transportations, thus the major responsibility of EVs' battery storage is sufficient power supply for driving cars. In order to have maximum satisfaction of customers and minimum grid disturbances, EVs' parking lots are actually a good promise to deal with the EVs' energy management challenges. So, parking lots are appropriate places for vehicle-to-grid (V2G) strategy implementation because EVs are typically parked 23 h each day in these places; and nearly 90% of vehicles are also parked even at the time of peak traffic hours [11]. EVs are equipped with batteries as an energy storage system to supply their electric-drive motors. Once EVs are plugged into the grid, they can operate in two different modes: charging mode (or G2V), and discharging mode (or V2G). In G2V mode, the EV acts as a load to the electric utility; while in V2G mode, EV could inject energy to the grid by discharging the energy stored in its battery. Thus, EVs may be manifested in load and/or generation unit from the utility grid viewpoint [12,13]. In V2G mode, depending upon the revenues and/or utility grid's demands, the state of charge (SOC) of an EV's battery may decrease/increase. In this mode, EV owners can make revenues when their cars are parked, providing great economic incentives for the owners. In V2G mode, on the other hand, utilities can benefit from an increased system flexibility and reliability as well as using energy storage for intermittent renewable energy resources (RESs).

A number of studies have been reported in the literature regarding optimal energy management of IPL to charge/discharge EVs in the IPL. In [14–16], only EVs scheduling schemes were proposed for a number of EVs in a parking lot without considering V2G capability. In [17], an approach with several objectives was proposed to allocate the optimum size of electrical energy to the EV parking with regard to peak demand, charging cost, and subscriber behavior. A new two-step technique was presented in [18] to find optimum site of EV parking lots and RESs with regard to the economic and technical constraints using population-based genetic algorithm (GA) and PSO algorithm. The obtained results revealed that remarkable cost reduction and network operational improvement were achieved by employing this method in simultaneous presence of EVs and RESs. Ref. [19] uses a two-stage energy management in order to minimize the distribution system's operation cost and the cost of IPLs for EVs regarding the load demand, generation limits, as well as charging/discharging constraints. In [20], a charging/discharging schedule was implemented in one IPL for the purpose of peak shaving and valley filling on load profile with regard to different EV places. Ref. [21] addresses an energy management to decrease the purchasing cost of energy in an IPL by shifting EV loads to fill the valley of total load demand. In [22], authors provided charging profiles of an IPL in different strategies (i.e., instant EVs charging, charging peak power minimization, and operational charging cost minimization). Ref. [23] provided a charging/discharging scheduling of plug-in hybrid electrical vehicles (PHEVs) at an IPL to maximize the IPL's owner profit, and at the same time, to consider the EV owners' constraints, including

final SOC.

In the literatures, different objective functions such as minimization of cost and air pollutant emission have been proposed for EVs management model. In addition, if the aggregated battery of EVs are considered as an energy storage system, another objective/goal may be appeared to maximize the aggregated batteries capability to suppress the intermittency of RESs [8–9]. Thus, most of the reported research determined optimum charging profile for EVs in one or some of the prelocated IPLs; some works, first, defined the charging profile of the EVs based on the prices. Next, on the basis of the specified charging profile, the optimum sites of IPLs were determined to optimize the cost and operation burden of distribution systems. These separated optimizations may result in non-global optimal solutions for the utility and EV owners.

The novelty of this paper is providing a new, simple and efficient formulation to manage an IPL with related considerations. The preferences of EV owners and constraints of the distribution system operation are formulated in this work that have not been usually considered in the optimizations of previous works. Additionally, optimum dispatching of a hydrogen storage system is considered to reduce the cost of IPLs. In this paper, an IPL with hydrogen unit, load demand and a bidirectional utility grid connection are presented for stochastic charging/discharging scheduling of PHEVs with the purpose of ensuring the SOC is acceptable and/or adequate for users at the time of departure. An energy management system is proposed here for IPL based on the hydrogen unit. Moreover, the proposed model observes the system constraints and customers' preferences. The problem of optimal energy management of IPL was solved using the particle swarm optimization (PSO) algorithm. The contributions of the paper are highlighted as follows:

- Include and aggregate hydrogen unit with EVs charging/discharging scheduling.
- Use IPL for possible interaction among EVs and upstream grid operator.
- Determine charge/discharge decisions of electrolyzer and fuel cell in HSS to decrease IPL operational cost.
- Evaluate EVs role in acting in two modes of storage/load.
- Consider the preferences of EVs owners in the related energy management program.
- Use PSO to model the problem with guaranteed global optimum solutions.

The rest of the paper is organized as follows: Section 2 presents the IPL model along with the components. Then, this section details the problem formulation as well as different constraints related to the EVs and utility. Simulation and analysis of results are presented in Section 3, followed by the conclusions in Section 4.

2. Intelligent parking lot (IPL) model

The structure of the proposed intelligent parking lot (IPL) system is shown in Fig. 1. As can be seen, this IPL consists of a hydrogen storage system (HSS), PHEVs, and load demand. This structure is considered for a designed system. The system is single-bus, and it is assumed that power flow equations are established and other constraints were neglected. This IPL participates in the day-ahead pool market (distribution level market), and the manager of the IPL exchanges energy with an upstream grid by participating in the day-ahead pool market. It is assumed that the IPL is a price-taker and could not have any effect on the market price and the market price for the day ahead is predicted.

2.1. Operation model of the hydrogen storage system

The hydrogen storage system consists of an electrolyzer, a fuel cell, and a hydrogen storage tank that are explained in detail as follows

2.1.1. Electrolyzer

The electrolyzer was used for splitting water into H_2 and O_2 elements by supplying a direct current to its electrodes.

The output power of the electrolyzer in every period t, $P^t_{EL-Tank}$, can be calculated using (1) [24]:

$$P^t_{EL-Tank} = P^t_{IPL-EL} * \eta_{EL} \quad (1)$$

where P^t_{IPL-EL} is the electrical power delivered to the electrolyzer from the IPL, and η_{EL} is electrolyzer efficiency.

Fuel cell: The fuel cell converts hydrogen energy into electrical energy by oxidizing H_2. The input power of the fuel cell is calculated using (2).

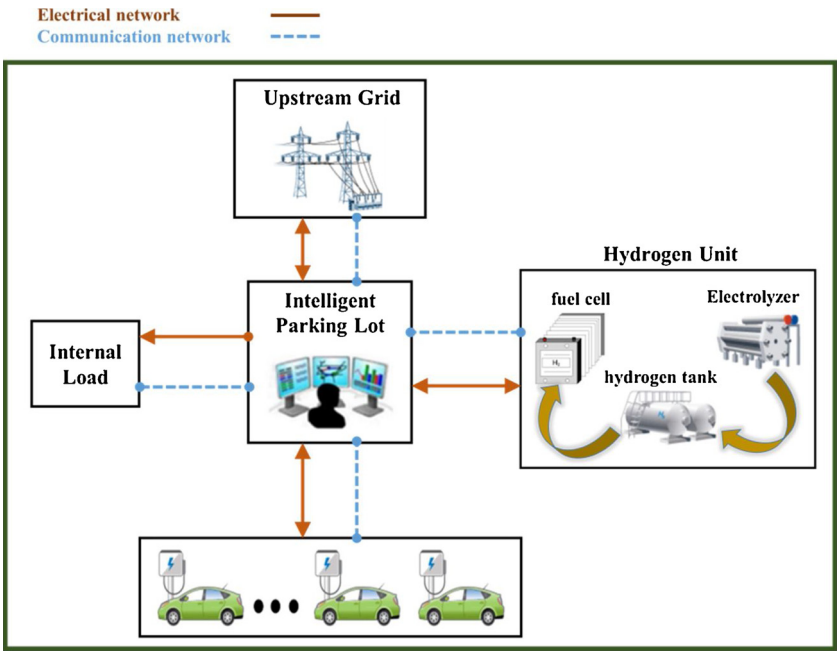

Fig. 1. The structure of the proposed IPL used in this study.

$$P^t_{Tank-FC} = \frac{P^t_{FC-IPL}}{\eta_{FC}} \quad (2)$$

where P^t_{FC-IPL} is the power transferred from the fuel cell to the IPL, and η_{FC} is fuel cell efficiency.

2.1.2. Hydrogen storage tank

The hydrogen produced by the electrolyzer is compressed and then stored in a pressurized tank. The rate of hydrogen stored in the tank and the rate of hydrogen being discharged from the tank into the fuel cell are calculated by (3) and (4), respectively [24].

$$H^t_{EL-Tank} = \frac{P^t_{EL-Tank}}{E_{H_2}} \quad (3)$$

$$H^t_{Tank-FC} = \frac{P^t_{Tank-FC}}{E_{H_2}} \quad (4)$$

where E_{H_2} is hydrogen energy per kg (kWh/kg). The energy stored in the tank in each period can be calculated via (5):

$$M^t_{Tank} = M^{t-\Delta t}_{Tank} + (H^t_{EL-Tank} - H^t_{Tank-FC} \times \eta_{Tank}) \times \Delta t \quad (5)$$

where M^t_{Tank} and $M^{t-\Delta t}_{Tank}$ are the hydrogen mass stored in the tank in periods t and t-Δt, respectively. Also, Δt is the length of each period and is equal to one hour, and η_{Tank} is the efficiency of the tank [24].

2.2. Model of PHEVs

The PHEVs are capable of operating in the grid-to-vehicle (G2V) or vehicle-to-grid (V2G) modes. In this study, the owners of the PHEVs are encouraged through some incentives offered by the IPL manager to participate in the V2G program. The PHEVs participating in this program are called V2G vehicles, and those which refrain from participating are labeled G2V vehicles.

For the periods the PHEVs are connected to the IPL, the SOC for each PHEV (SOC^t_v) depends on the SOC of the vehicle in a previous period ($SOC^{t-\Delta t}_v$) and its current charging/discharging state as modeled in (6) [25].

$$SOC^t_v = SOC^{t-\Delta t}_v + \left(\frac{\eta^v_c P^t_{v.c}}{C^v} - \frac{P^t_{v.d}}{\eta^v_d C^v}\right) \times \Delta t \; ; \; t^a_v < t \le t^d_v \quad (6)$$

where $P^t_{v.c}$ and $P^t_{v.d}$ are the charging and discharging power of the battery, respectively. Also, η^v_c and η^v_d are the charging and discharging efficiencies of the battery, respectively. Moreover, C^v is the capacity of the battery, and finally t^a_v and t^d_v are the arrival and departure times, respectively.

2.2.1. The revenues/costs of the IPL engaged in interactions with the PHEVs

The IPL under discussion has the following revenues and costs due to its interactions with the PHEVs:

- Revenue from selling energy to the G2V vehicles
- Revenue from selling energy to the V2G vehicles
- The cost of purchasing energy from the V2G vehicles
- The cost of using the available capacity of the V2G vehicles
- The penalty cost of failure to satisfy the charging requirements of the V2G vehicles

Revenue from selling energy to the G2V vehicles is calculated via (7) [26]:

$$R^t_{PHEV-m_{G2V}} = \sum_{v=1}^{m_{G2V}} (P^t_{v.c} \times \rho^t_c) \times \Lambda^t_v \times \Delta t \quad (7)$$

where $P^t_{v.c}$ is the charging power of the vehicle, ρ^t_c is the charging price of the vehicle in period t, and Λ^t_v is a binary variable that shows the connection state of the vehicle in every period.

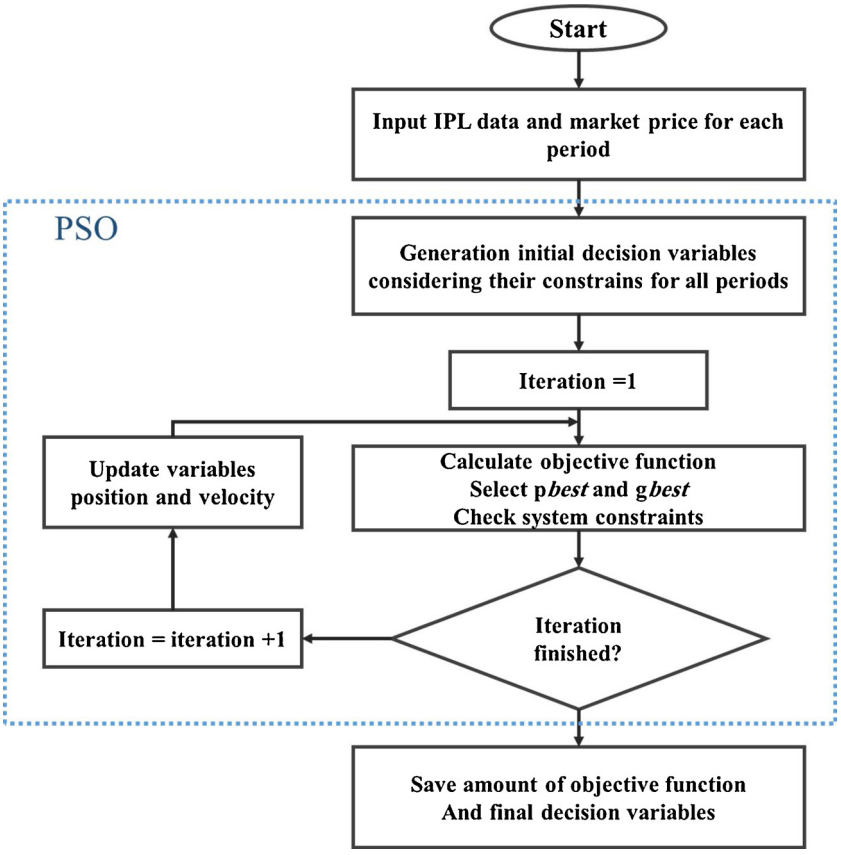

Fig. 2. The simulation flowchart.

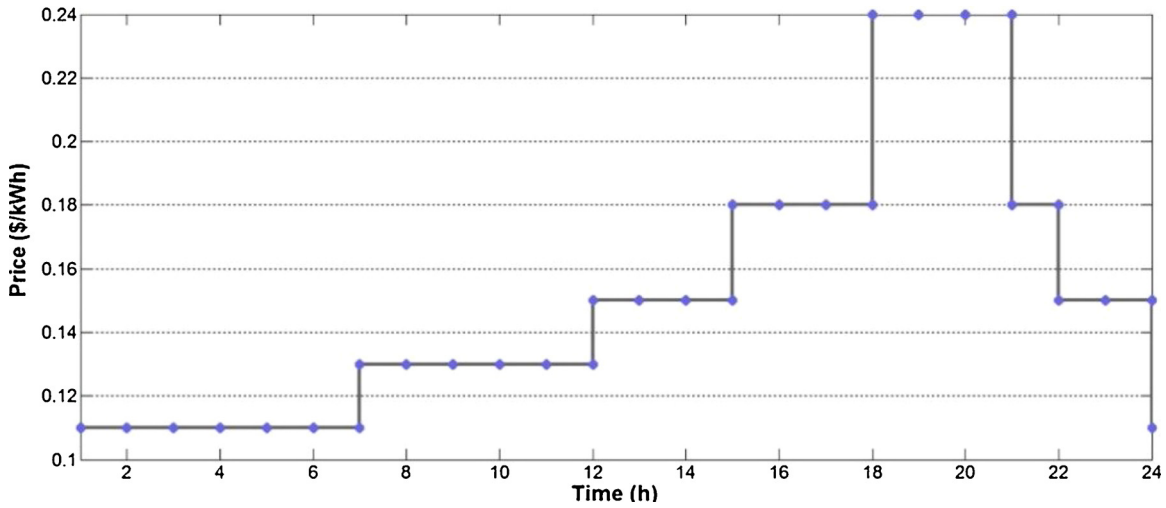

Fig. 3. Forecast market price profile [27].

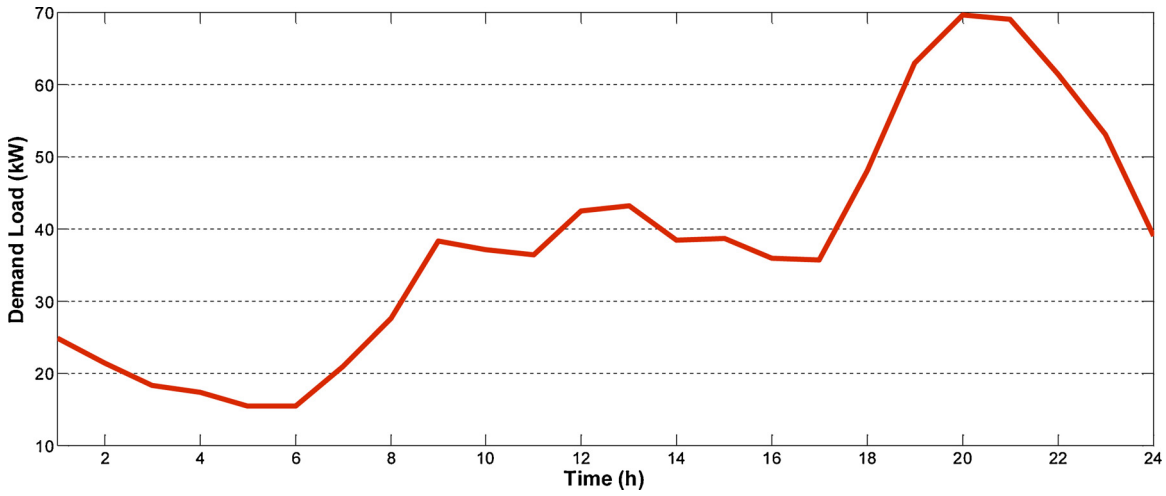

Fig. 4. MCS results for load demand.

Table 1
The technical specifications of the hydrogen unit [24].

P_{El-max}	P_{FC-max}	$M_{Tank-max}$	$M_{Tank-min}$	$M_{Tank-initial}$	E_{H_2}
kW	*kW*	*kg*	*Kg*	*kg*	*kWh/kg*
40	20	8	1.25	5	39.7

For the V2G vehicles, the SOC at departure time ($SOC_{t_v^d}$) shows whether the vehicle is a buyer or a seller of energy. If this final SOC is smaller than the initial SOC, then vehicle is the seller, but if it is larger than the initial SOC, then the vehicle is the buyer.

Revenue from selling energy to the V2G vehicles is calculated using (8).

Table 3
The technical characteristics of the PHEVs [31].

PHEV	Battery Lithium-Ion	η_c^v	η_d^v	SOC_{min}	SOC_{max}
	kWh	%	%	%	%
NISSAN LEAF®	24	90	95	15	95

$$R^t_{PHEV-m_{V2G}} = \sum_{v=1}^{m_{V2G}} (SOC_{t_v^d} - SOC_{t_v^a}) \times C^v \times \rho^t_{c.V2G} \times \tau_v^d \quad (8)$$

where $SOC_{t_v^d}$ and $SOC_{t_v^a}$ are the final and initial SOC of the vehicle, respectively. Also, $\rho^t_{c.V2G}$ is the charging price of the V2G vehicle in period *t*, m_{V2G} is the set of V2G vehicles, and τ_v^d is the flag that indicates the departure time of the vehicle.

Table 2
The economic characteristics of components [30].

IPL components	Lifetime	Initial investment cost	Capacity factor	Maintenance costs	Efficiency
	n	A	CF	C_m	??
	Year	*$/kW*	%	*$/year*	%
Fuel cell	13	700	0.9	20	50
Electrolyzer	15	350	0.9	25	75
Hydrogen tank	20	625($/kg)	0.9	15	95

Table 4
The charge and discharge Tariff of the PHEVs.

ρ_c^t	$\rho_{c,V2G}^t$	$\rho_{d,V2G}^t$	$\rho_{cap,V2G}^t$	$\rho_{Penalty}$
\$/kWh	\$/kWh	\$/kWh	\$/kWh	\$/kWh
$1.3\times\rho_{grid}^t$	$1.1\times\rho_v^{plug-in}$	$1\times\rho_v^{plug-in}$	$0.02\times\rho_{grid}^t$	$4\times\rho_v^{plug-in}$

$\rho_v^{plug-in}$: equal to the average market price during the periods each PHEV is connected to the.

Table 5
The desired SOC of the V2G PHEVs.

PHEV (v)	1	2	3	4	5	6	7	8	9	10
$SOC_v^{desired}$ (%)	90	60	90	85	75	75	55	70	90	60

Table 6
The predicted data of the G2V PHEVs.

PHEV (v)	t_a^v	t_d^v	$SOC_{t_a}^v$
1	7:13	13:11	45.59
2	9:10	15:20	22.04
3	9:35	15:50	27.3
4	7:35	18:50	40.36
5	12:07	21:45	16.47

Table 7
The predicted data of the V2G PHEVs.

PHEV (v)	t_a^v	t_d^v	$SOC_{t_a}^v$
1	7:10	15:33	50
2	8:55	17:55	31.6
3	6:20	15:25	42.9
4	8:12	16:43	48.2
5	8:05	13:46	42.5
6	7:46	17:05	37.8
7	9:55	13:40	48.5
8	5	16:30	33
9	6:10	14:40	63
10	7:42	13:50	46.3

If the final SOC is smaller than the initial SOC, the cost of purchasing energy from the V2G vehicles is obtained from (9).

$$C_{PHEV-mV2G}^t = \sum_{v=1}^{m_{V2G}} (SOC_{t_v^a} - SOC_{t_v^d}) \times C^v \times \rho_{d,V2G}^t \times \tau_v^d \tag{9}$$

where $\rho_{d.V2G}^t$ is the discharging price of the V2G vehicles in period t.

Furthermore, the manager imposes some cost for using the available capacity per hour of the V2G vehicles (i.e., the incentive discussed above). This cost is calculated using (10) [26]:

$$C_{Cap-V2G}^t = \sum_{v=1}^{m_{V2G}} (SOC_v^{max} - SOC_v^{min}) \times C^v \times \rho_{cap,V2G}^t \times \Lambda_v^t \tag{10}$$

where SOC_v^{max} and SOC_v^{min} are the maximum and minimum SOC of the vehicle, respectively, and $\rho_{cap,V2G}^t$ is the price of the available capacity in period t.

If the actual final SOC is less than the desired final SOC, the manager is committed to pay the penalty cost of failure to meet the charging requirements of the V2G vehicles. This cost is obtained from (11) as follows:

$$C_{Penalty}^t = \sum_{v=1}^{m_{V2G}} (SOC_v^{desired} - SOC_v^{t_d}) \times C^v \times \rho_{Penalty} \times \tau_v^d \; if \; : SOC_v^{t_d} < SOC_v^{desired} \tag{11}$$

where $SOC_v^{desired}$ is the desired final SOC of the vehicle, and $\rho_{Penalty}$ is the tariff of the penalty cost.

3. Objective function

3.1. Decision variables

The decision variables for each period are the power exchanged with the upstream grid (P_{grid}^t), the charging or discharging power of ten V2G PHEVs and five G2V PHEVs (P_v^t), and the power exchanged with the hydrogen unit (P_H^t). Thus, there are 17 decision variable vectors for each period and 408 variables for the study day as follows (12):

$$\mathcal{X} = \begin{bmatrix} P_{grid}^1 \; P_{v1}^1 \; P_{v2}^1 \ldots P_{mg2v}^1 \ldots P_{mv2g}^1 \; P_H^1 \\ P_{grid}^2 \; P_{v1}^2 \; P_{v2}^2 \ldots P_{mg2v}^2 \ldots P_{mv2g}^2 \; P_H^2 \\ \vdots \\ P_{grid}^{24} \; P_{v1}^{24} \; P_{v2}^{24} \ldots P_{mg2v}^{24} \ldots P_{mv2g}^{24} \; P_H^{24} \end{bmatrix} \tag{12}$$

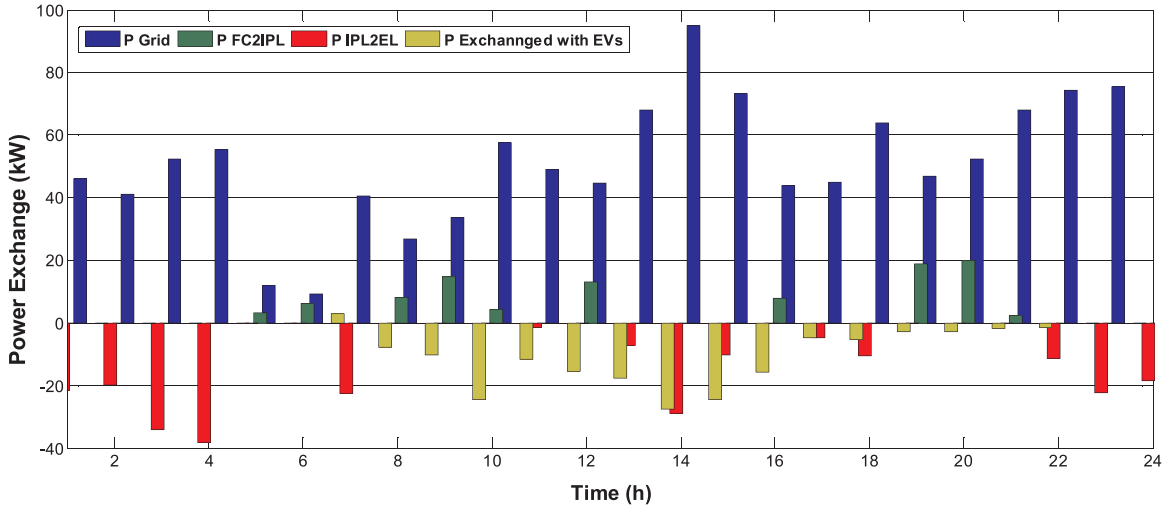

Fig. 5. The results of scheduling.

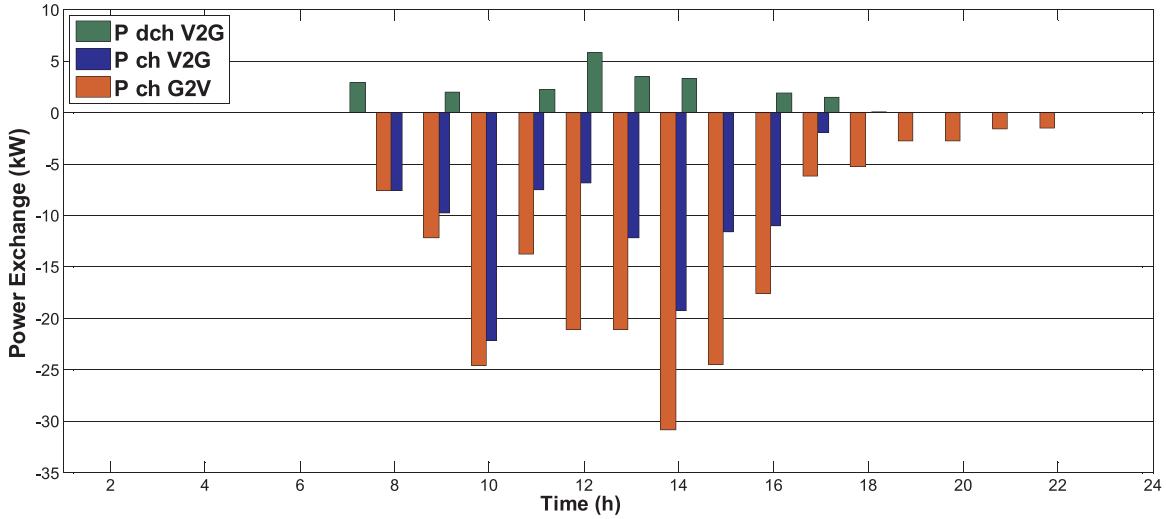

Fig. 6. The charging and discharging power of the PHEVs.

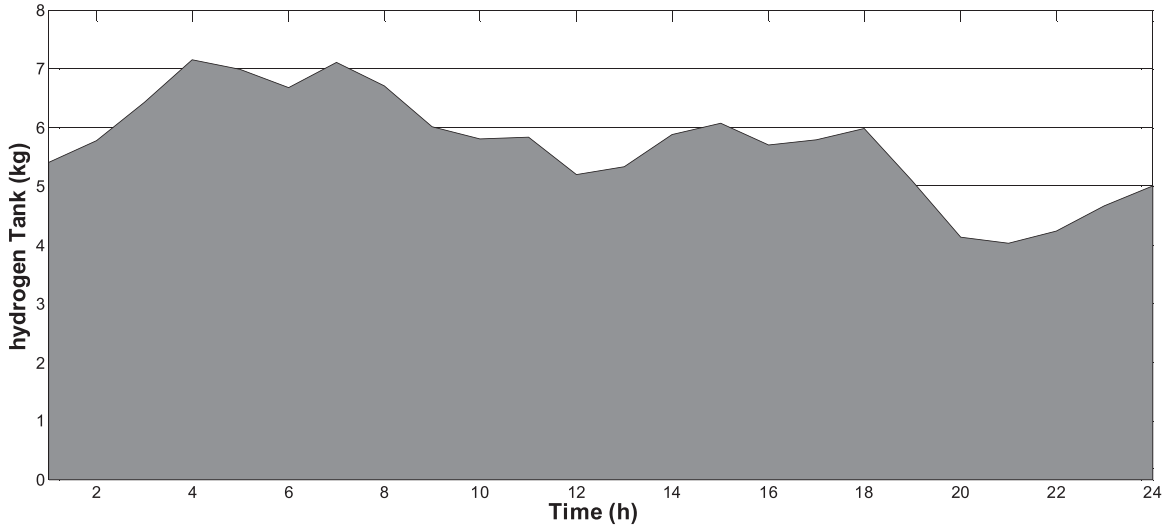

Fig. 7. The level curve of the hydrogen stored in the tank.

3.2. Profit function

The profit function of the IPL is computed by adding up the difference between the revenues and the costs in all periods and is formulated using (13):

$$Profit = \sum_{t=1}^{T=24} \begin{bmatrix} ((P^t_{sell-grid} \times \rho^t_{grid}) - (P^t_{buy-grid} \times \rho^t_{grid})) \times \Delta t \\ + (\rho^t_{sell-load} \times P^t_L) \times \Delta t \\ + (R^t_{PHEV-mG2V} + R^t_{PHEV-mV2G}) \\ - (C^t_{PHEV-mV2G} + C^t_{Cap\_V2G} + C^t_{Penalty}) \\ - (C_{FC}(t) + C_{EL}(t) + C_{Tank}(t)) \end{bmatrix} \quad (13)$$

where $P^t_{sell-grid}$ and $P^t_{buy-grid}$ are the power sold and purchased to/from the upstream grid, respectively. If power flows from the upstream grid to the IPL, $P^t_{buy-grid}$ is equal to P^t_{grid} and $P^t_{sell-grid}$ is zero. In contrast, if power flows from the IPL to the upstream grid, $P^t_{sell-grid}$ is equal to P^t_{grid} and $P^t_{buy-grid}$ is zero. P^t_L is electrical load in period t and $\rho^t_{sell-load}$ is the price at which the IPL sells energy to its loads. C_{FC}, C_{EL}, and C_{Tank} are the operation/maintenance costs of the fuel cell, electrolyzer, and hydrogen tank, in that order.

It is assumed that the uncertainties in load demand and the driving patterns of PHEVs were modeled using the probability distribution function and the Monte Carlo simulation (MCS) separately, and the certain values of these parameters are considered in the calculations [27].

The objective function is solved considering constraints so as to maximize the profit function. This is represented in (14).

$$OF = \max_{\mathscr{X}}(Profit) \quad (14)$$

3.3. Constraints

It is assumed that the IPL is connected to an upstream grid in one bus, and the objective functions are optimized considering the following constraints (15)–(21) [24,27–29].

$$P^t_{IPL-EL} + P^t_L + P^t_c + P^t_{sell-grid} = P^t_{FC-IPL} + P^t_{buy-grid} + P^t_d \quad (15)$$

$$P^t_{grid};\ |P^t_{grid}| \le P_{grid\_max} \quad (16)$$

$$SOC^{min}_v \le SOC^t_v \le SOC^{max}_v \quad (17)$$

$$-P^{max}_{v,d} \le P^t_v \le P^{max}_{v,c} \quad (18)$$

$$-P^{max}_{EL} \le P^t_H \le P^{max}_{FC} \quad (19)$$

$$M^t_{Tank} \le M_{max} \quad (20)$$

$$M_{Tank}^{0} = M_{Tank}^{24} \tag{21}$$

In the IPL power balance constraint (15), P_c^t and P_d^t respectively denote the sum of the charging and discharging power of all the PHEVs in period *t*. In (16), P_{grid_max} is the maximum capacity of the transmission line connected to the upstream grid. Constraint (17) ensures that the energy charged to the battery and the energy discharged from it is lower than the empty capacity and the energy content of the battery, respectively. In (18), $P_{v.c}^{max}$ and $P_{v.d}^{max}$ are the maximum charging and discharging power of the charger, respectively. In the hydrogen unit constraints, (19) and (20), P_{EL}^{max} and P_{FC}^{max} are the maximum power of the electrolyzer and the fuel cell, respectively, and M_{max} is the maximum capacity of the hydrogen tank. In (21), it is assumed that the mass of hydrogen in the tank at the end of the operation period should be equal to the mass of hydrogen at the beginning of the study day. This is because enough hydrogen should be available on the following day for operation. The operation and maintenance cost of IPL components are calculated by (22) as follows [27]:

$$C^t = \left(\frac{\left(\frac{\gamma(1+\gamma)^n}{(1+\gamma)^n - 1} \right) \times A}{CF \times 8760 \times P_{rated}} \times P^t + C_M \right) \tag{22}$$

where for each component, C_M is the maintenance cost ($/year), CF is the capacity factor, A is the initial investment cost ($), n is the lifetime, and γ is the interest rate. In addition, P_{rated} and P^t are the rated power and actual power of each component, respectively.

4. Simulations and discussion

The model proposed for the optimal operation of the IPL was solved using MATLAB software running on a PC with an AMD Processor A10 (2.5 GHz) and 8 GB of RAM. The simulation flowchart is depicted in Fig. 2.

First, the certain value of the load demand, and the driving pattern of the PHEVs in each period were placed in the profit function in (13). Then, the objective function in (14) was solved using the PSO algorithm [29] in order to provide the scheduling of the optimal operation of the IPL.

4.1. Input data

The profile of the forecast market price is depicted in Fig. 3. Also, the certain values of load demand are illustrated in Fig. 4.

Considering the subscription fee, $\rho_{sell-load}^t$ was assumed to be 30% more than the market price, and the interest rate was considered 5%. The technical characteristics of the hydrogen unit and the economic characteristics of IPL components are provided in Tables 1 and 2, respectively.

The number of EVs participating at V2G program is 10; and, the number of EVs visited parking lot during the day for optional charging (unscheduled) is 5.

All the PHEVs used in the present study had the same characteristics. The technical characteristics of the PHEVs are given in Table 3. The maximum power of the charger used to charge and discharge in the case of each PHEV was considered 4 kW. Table 4 gives the charging tariff of the G2V vehicles together with the charging and discharging tariff, available capacity tariff, and penalty tariff of the V2G vehicles. The desired SOC of the V2G vehicles at the time of departure is presented in Table 5.The predicted values of arrival time, departure time, and initial SOC are provided in Table 6 (G2V vehicles) and Table 7 (V2G vehicles).

Standard deviation (SD) of arrival/departure times is considered in *hr* and the mean and SD of initial energy level of EV battery is considered in %.

4.2. Results of simulation

Fig. 5 displays the scheduling results of the interactions of the IPL with the PHEVs, upstream grid, fuel cell, and electrolyzer. The IPL profit turned out to be $ 17.2 and as can be seen, the IPL purchase power from the upstream grid in all periods of the study day.

The gained revenue of power selling to the electrical loads is $ 193.46. The amount of energy purchased from upstream network is declined at 5th and 6th hours considering the reduced load of parking lot and absence of EVs at the parking lot. The amount of hydrogen stored in storage tank is increased at 1st and 4th hours by utilizing the electrolyzer considering reduce energy price and vacancy of parking lot.

The charge and discharge of the PHEVs is displayed in Fig. 6. Obviously, the parking was employed in periods 7 to 22, and it interacted with the IPL. The total energy sold to the G2V vehicles was 83.46 kW h. These vehicles were regarded as sensitive loads, and the revenue earned from them was $ 18.25. The revenue from selling energy to the V2G vehicles, the cost of available capacity, and the overall profit of these vehicles were $ 9.53, $ 4.22, and $ 5.31, respectively. The penalty cost is zero because the charging requirements of the V2G vehicles are satisfied.

Based on the output data of time 12, the amount of parking lot consumption load is 42.42 kW; while, the amount of power purchased from upstream network is 44.55 kW. And, the amount of power produced by fuel cell is 13.18 kW; finally, the net power exchanged between vehicles and parking lot at this time is 15.31 kW (injected to the parking lot). At this time, the amount of power charged to EVs participating at V2G program is 6.9 kW; and, the amount of discharged power is 578 kW; the amount of power charged to EVs participating at G2V program is 14.18 kW. The level curve of the hydrogen stored in the tank is shown in Fig. 7. Obviously, at times the fuel cell is operated, the amount of hydrogen available in the tank is reduced. And, when the electrolyzer is operated, the hydrogen level is increased. For example, between times 1–4 when the eloctrolyzer is operated, the amount of hydrogen stored in the tank is increased from the initial amount of 5 kg to 7.14 kg. However, between 18–21 hr, with the operation of fuel cell, the amount of hydrogen is decreased from 5.98 to 4.01 kg. It can be seen that at the end of the operation periods, hydrogen in the tank was equal to the mass of hydrogen at the beginning of the study day. This is because enough hydrogen should be available in the next day for operation.

5. Conclusions

This paper developed a new model for the charging/discharging of PHEVs. Also, this paper used a hydrogen unit as a storage unit for IPL. The proposed formulation is uncomplicated and it was applied to a designed IPL system. The numerical results verified the effectiveness of the proposed method. In this paper, a probabilistic method was employed for charging/discharging management in electrical vehicles for optimal operation of parking lot at each time under electrical load uncertainty, market price, as well as driving pattern of EVs. The use of hydrogen storage resulted in system usefulness. The obtained result revealed that the proposed algorithm is economically efficient. And, EVs charge/discharge, power sold/bought to/from upstream network, as well as utilization of hydrogen unit using the proposed algorithm are determined for maximized profit.

References

[1] A. Salehabadi, F. Sarrami, M. Salavati-Niasari, T. Gholami, D. Spagnoli, A. Karton, Dy3Al2(AlO4)3 ceramic nanogarnets: sol-gel auto-combustion synthesis, characterization and joint experimental and computational structural analysis for electrochemical hydrogen storage performances, J. Alloys Compd. (2018), https://doi.org/10.1016/j.jallcom.2018.02.117.

[2] S. Nojavan, K. Zare, Interval optimization based performance of photovoltaic/wind/FC/electrolyzer/electric vehicles in energy price determination for customers

by electricity retailer, Sol. Energy 171 (September 1) (2018) 580e92.
[3] S.M. Hakimi, S.M. Moghaddas-Tafreshi, Effect of plug-in hybrid electric vehicles charging/discharging management on planning of smart microgrid, J. Renew. Sustain. Energy 4 (6) (2012) 1–14.
[4] M. Pantos, Stochastic optimal charging of electric-drive vehicles with renewable energy, Energy 36 (11) (2011) 6567–6576.
[5] F. Basrawi, T.K. Ibrahim, K. Habib, T. Yamada, Effect of operation strategies on the economic and environmental performance of a micro gas turbine trigeneration system in a tropical region, Energy 97 (2016) 262–272.
[6] A.G. Anastasiadis, S.A. Konstantinopoulos, G.P. Kondylis, G.A. Vokas, P. Papageorgas, Effect of fuel cell units in economic and environmental dispatch of a Microgrid with penetration of photovoltaic and micro turbine units, Int. J. Hydrogen Energy 42 (February (5)) (2017) 3479–3486.
[7] H. Kikusato, et al., Electric vehicle charge-discharge management for utilization of photovoltaic by coordination between home and grid energy management systems, IEEE Trans. Smart Grid (2018).
[8] Ali Salehabadi, Masoud Salavati-Niasari, Tahereh Gholam, Green and facial combustion synthesis of Sr3Al2O6 nanostructures; a potential electrochemical hydrogen storage material, J. Clean. Prod. (2017), https://doi.org/10.1016/j.jclepro.2017.09.250.
[9] Rodolfo Dufo-Lo´ peza, L. Bernal-Agustı´na Jose´, Javier Contrerasb, Optimization of control strategies for stand-alone renewable energy systems with hydrogen storage, Renew. Energy 32 (2007) 1102–1126.
[10] Maryam Ghiyasiyan-Arani, Masoud Salavati-Niasari, Effect of Li2CoMn3O8 nanostructures synthesized by combustion method on montmorillonite K10 as a potential hydrogen storage material, J. Phys. Chem. (2018), https://doi.org/10.1021/acs.jpcc.8b02617.
[11] S. Shahidinejad, S. Filizadeh, E. Bibeau, Profile of charging load on the grid due to plug-in vehicles, IEEE Trans. Smart Grid 3 (1) (2012) 135–141.
[12] S. Rezaee, E. Farjah, B. Khorramdel, Probabilistic analysis of plug-in electric vehicles impact on electrical grid through homes and parking lots, IEEE Trans. Sustain. Energy 4 (4) (2013) 1024–1033.
[13] M. Honarmand, A. Zakariazadeh, S. Jadid, Optimal scheduling of electric vehicles in an intelligent parking lot considering vehicle-to-grid concept and battery condition, Energy 65 (2014) 572–579.
[14] W. Su, M.Y. Chow, Performance evaluation of an EDA-based large-scale plug-in hybrid electric vehicle charging algorithm, IEEE Trans. Smart Grid 3 (1) (2012) 308–315.
[15] G.B. Shrestha, S.G. Ang, A study of electric vehicle battery charging demand in the context of Singapore, Proceedings of International Power Engineering Conference (2007) 64–69.
[16] K. Mets, T. Verschueren, W. Haerick, C. Develder, F.D. Turck, Optimizing smart energy control strategies for plug-in hybrid electric vehicle charging, Proceedings of IEEE/IFIP Network Operation Management Symposium (NOMS), Osaka, Japan, 2010, pp. 293–299.
[17] A. El-Zonkoly, Intelligent energy management of optimally located renewable energy systems incorporating PHEV, Energy Convers. Manage. 84 (2014) 427–435.
[18] M.H. Amini, M. Parsa Moghaddam, O. Karabasoglu, Simultaneous allocation of electric vehicles' parking lots and distributed renewable resources in smart power distribution networks, Sustain. Cities Soc. 28 (2017) 332–342.
[19] S. Aghajani, M. Kalantar, Operational scheduling of electric vehicles parking lot integrated with renewable generation based on bilevel programming approach, Energy 139 (2017) 422–432.
[20] C.S. Ioakimidis, D. Thomas, P. Rycerski, K.N. Genikomsakis, Peak shaving and valley filling of power consumption profile in non-residential buildings using an electric vehicle parking lot, Energy 148 (2018) 148–158.
[21] K. Seddig, P. Jochem, W. Fichtner, Integrating renewable energy sources by electric vehicle fleets under uncertainty, Energy 141 (2017) 2145–2153.
[22] N.G. Paterakis, M. Gibescu, A methodology to generate power profiles of electric vehicle parking lots under different operational strategies, Appl. Energy 173 (2016) 111–123.
[23] M.J. Mirzaei, A. Kazemi, O. Homaee, RETRACTED: real-world based approach for optimal management of electric vehicles in an intelligent parking lot considering simultaneous satisfaction of vehicle owners and parking operator, Energy 76 (2014) 345–356.
[24] Soheil Mohseni, Seyed Masoud Moghadas-Tafreshi, A multi-agent system for optimal sizing of a cooperative self-sustainable multi-carrier microgrid, Sustain. Cities Soc. 38 (April 2018) (2018) 452–465.
[25] Alireza Soroudi, Andrew Keane, Chapter 5, "Risk averse energy hub management considering plug-in electric vehicles using information gap decision theory,", Plug-In Electric Vehicles in Smart Grids, Springer, Singapore, 2015.
[26] Masoud Honarmand, Alireza Zakariazadeh, Shahram Jadid, Self-scheduling of electric vehicles in an intelligent parking lot using stochastic optimization, J. Franklin Inst. 352 (2) (2014) 449–467.
[27] Reza Jabbari-Sabet, Seyed-Masoud Moghaddas-Tafreshi, Seyed-Sattar Mirhoseini, Microgrid operation and management using probabilistic reconfiguration and unit commitment, Electr. Power Energy Syst. 75 (2016) 328–336.
[28] Seyed Masoud Moghaddas Tafreshi, Hassan Ranjbarzadeh, Mehdi Jafari, Hamid Khayyam, A probabilistic unit commitment model for optimal operation of plug-in electric vehicles in microgrid, Renew. Sustain. Energy Rev. 66 (2016) 934–947.
[29] M. Shahverdi, S.M. Moghaddas-Tafreshi, Operation optimization of fuel cell power plant with new method in thermal recovery using particle swarm algorithm, Proc. 3rd International Conference on DRPT, (2008), pp. 2542–2547.
[30] D. Steward, G. Saur, M. Penev, T. Ramsden, "Lifecycle Cost Analysis of Hydrogen Versus Other Technologies for Electrical Energy Storage," Technical Report, NREL/TP-560-46719, November (2009).
[31] Alireza Zakariazadeh, Shahram Jadid, Pierluigi Siano, Integrated operation of electric vehicles and renewable generation in a smart distribution system, Energy Convers. Manage. 89 (2015) 99–100.